

## Surface properties of clean, and with adsorbed oxygen, surfaces of CdTe (110), {111}, and (100) and of CdSe {0001} studied by electron-energy-loss spectroscopy and Auger-electron spectroscopy

Atsuko Ebina, Kiyomitsu Asano, and Tadashi Takahashi

*Research Institute of Electrical Communication, Tohoku University, Sendai 980, Japan*

(Received 4 December 1979; revised manuscript received 21 March 1980)

Surface electronic states and oxidation properties of CdTe (110), {111}, and (100) surfaces and CdSe {0001} surfaces have been studied with low-energy electron-loss spectroscopy, Auger-electron spectroscopy, and low-energy-electron diffraction. The surface losses due to the transitions from the Cd-4*d* core level locate the empty Cd-derived surface states at 2.5 [for the (110) and (111) plane] or 3.0 eV [for the (100)] in CdTe and 2.7 eV in CdSe, with respect to the valence-band maximum. The losses appearing at 61 and 66.2 eV in CdSe are identified as due to the transitions from the Se-3*d* core level to the Se-derived surface states lying at about 8 and 13 eV above the valence-band maximum. No corresponding Te-derived empty surface states, i.e., transitions from the Te-4*d* level to Te-derived surface states, have been detected for CdTe. Oxygen uptake on the ordered surface is very slow when the surface is exposed to molecular oxygen; the initial sticking coefficients are  $10^{-13}$  for CdTe (100), less than  $10^{-14}$  for CdTe (110), and  $10^{-14}$  for CdSe (0001). Oxidation is stimulated drastically by electron-beam irradiation on the surface exposed to molecular oxygen and bulklike oxide overlayers are formed. Upon oxidation of CdTe surfaces, the shifted Te-4*d* loss due to TeO<sub>2</sub> occurs at rather early stages of oxidation and grows in magnitude with oxygen uptake, and the loss spectrum from the heavily oxidized surface resembles that of TeO<sub>2</sub>, while formation of neither a CdO nor a Cd element is evident. These findings indicate that the oxygen adsorbs preferentially on surface Te atoms by breaking the back bonds at the initial stages of oxidation, and then oxidation proceeds into the bulk, forming the oxide overlayer composed entirely of TeO<sub>2</sub>. In the case of the CdSe (0001) surface, oxygen adsorbs only on the surface Se atoms without breaking the back bonds at the initial stages of oxidation, and then it seems to adsorb with a breaking of the back bonds, and both selenium oxide and cadmium oxide are formed, although part of the selenium oxide sublimates away from the surface, leaving the oxide overlayer rich in CdO.

### I. INTRODUCTION

We have been investigating in the past several years electron-energy-loss spectra of low-index surfaces of ZnSe, ZnTe, and CdTe,<sup>1-3</sup> and have tried to determine the energy position of the surface state involved in the transitions from the cation (Zn and Cd) and anion (Se and Te) *d* core levels. The results show that the empty cation-derived surface state of these compounds lies above the bottom of the conduction band; i.e., there are no empty surface states in the band-gap region. We demonstrated also that oxygen uptakes on these surfaces were less than one monolayer coverage after exposing well-ordered surfaces to molecular oxygen, but electron-beam irradiation during the course of measurements of energy-loss and Auger-electron spectra stimulated oxidation and true bulklike oxides were formed by beam irradiation on the surface exposed to oxygen. Oxidation of ZnSe and ZnTe contained both cation and anion oxides, while sublimation of the volatile anion oxides of SeO<sub>2</sub> and TeO<sub>2</sub> led to a formation of the bulklike oxide overlayer composed entirely of ZnO on the very heavily oxidized surface of the Zn compounds. In the case of CdTe a formation of the bulklike anion oxide was evidenced by comparing a loss spectrum of the oxidized surface with that of TeO<sub>2</sub> (Ref. 3), but the detailed chemical composition of the oxide over-

layer has been undetermined as yet because of a possible presence of the cation oxide and/or the Cd element in the oxide layer.

In the present paper we will report in detail on the energy-loss spectroscopy (ELS) of (110), {111}, and (100) surfaces of CdTe and {0001} surfaces of CdSe. Cleanliness and orderliness of the surface are examined with Auger electron spectroscopy (AES) and low-energy-electron diffraction (LEED). CdTe itself is of interest in a systematic understanding of surface properties of II-VI compounds. In addition, we expected that oxidation of CdSe might lead to a formation of the bulklike CdO layer, and the resulting loss data could provide valuable information for deeper understanding of oxidation properties of the cation in CdTe. The present results on the clean and oxidized surfaces of CdTe and CdSe will be compared with those on the Zn compound surfaces reported previously.

### II. EXPERIMENTAL

Single crystals of *n*- and *p*-type CdTe grown from the melt and of *n*-type CdSe obtained from Eagle-Picher Inc. were employed. The x-ray oriented {111}, (100), and {0001} surfaces were chemically polished with a K<sub>2</sub>Cr<sub>2</sub>O<sub>7</sub>-HNO<sub>3</sub> solution at room temperature for about 2 min and then were treated with a NaOH solution at 50 °C for

several seconds. The (110) surface was prepared by cleaving the crystal in air just prior to introducing it into the chamber.

The experimental setup used in the present work is the same as that of our previous work.<sup>1-3</sup> The stainless-steel chamber is equipped with a 220-l/sec ion pump, a titanium sublimation pump, a single-pass cylindrical mirror analyzer (CMA) with a coaxial electron gun, a four-grid LEED optics, an Ar<sup>+</sup> sputtering gun, Bayard-Alpert (B-A) and extractor gauges, and a quadrupole mass filter. The base pressure of the chamber was  $1 \times 10^{-10}$  Torr and the working pressure was  $3 \times 10^{-10}$  Torr. On exposing the surface to oxygen, high-purity oxygen gasses were introduced in the chamber. To reduce contamination from the electron gun, it was necessary to preheat the filament of the gun for more than about 90 min after introducing oxygen gasses into the chamber.

Energy-loss and Auger spectra were measured with the CMA at primary electron-beam normal incidence on the surface and back-scattered electrons were detected with the CMA in a cone of 42° half aperture. The second derivative  $d^2N/dE^2$  of the energy-distribution curve was recorded for energy-loss spectroscopy (ELS) with modulation voltage  $\Delta V$  of 0.2 or 0.5 V peak to peak with primary electron energies  $E_p$ 's from 50 through 300 eV. In AES, the first derivative  $dN/dE$  was recorded with a primary electron energy of 2 keV and  $\Delta V$  of 1 V peak to peak for Auger electron energies below 200 eV, and 2 V peak to peak above 200 eV. The energy resolution in the loss spectrum was within 0.3 eV.

Clean surfaces were prepared by repeated cleaning by Ar<sup>+</sup> bombardment and annealing. Ordered surfaces without impurities within AES detection limits were provided except for the CdTe ( $\bar{1}\bar{1}\bar{1}$ ) and CdSe (000 $\bar{1}$ ) surfaces. While Ar<sup>+</sup> bombardment provided clean surfaces without any impurities, annealing led to contaminations with K on the polar anion surfaces. Repeated cycles of Ar<sup>+</sup> bombardment and annealing could not eliminate the K impurity. It diminished, however, with oxygen uptakes and disappeared on the heavily oxidized surface. The other commonly detected impurity is oxygen. The detection limit for the O impurity was about 0.01 of a monolayer coverage.

### III. RESULTS

#### A. CdTe

No significant differences were observed in energy-loss and Auger spectra and LEED patterns between the *n*- and *p*-type crystals except for the {111} surfaces. While oxygen impurities were eliminated below an AES detection limit, electron-

beam irradiation during ELS and AES measurements caused detectable oxygen contamination on the ( $\bar{1}\bar{1}\bar{1}$ ) and (100) surfaces. Contamination with oxygen was not detected on the ordered (111) surface on beam irradiation up to 80 min. For the ordered (110) surface, electron-beam-stimulated oxidation is not so remarkable as in the case of the ( $\bar{1}\bar{1}\bar{1}$ ) or (100) surface.

The (110) and (111) surfaces exhibit clean and well-defined  $1 \times 1$  and  $2 \times 2$  LEED patterns, respectively. The ( $\bar{1}\bar{1}\bar{1}$ ) surface of the *n*-type crystal displays a  $1 \times 1$  structure after annealing at 400 °C for 30 min. Subsequent annealing at 450 °C for 10 min does not produce any visual changes in LEED pattern, but further heating at a temperature between 450 and 550 °C offers a faceting pattern superimposed on a  $1 \times 1$  structure. The *p*-type crystal exhibits weak facets on a (111)  $2 \times 2$  surface and a faceting structure on the ( $\bar{1}\bar{1}\bar{1}$ ) surface. The (100) surface has a  $1 \times 3$  structure, where the periodicity of the unity is along the direction of the Cd broken bonds, if the surface is assumed to be a Cd-terminating one.

The oxygen uptake of the ordered (110) surface is extremely slow for exposures to molecular oxygen; no detectable oxygen Auger signal was noticed after 2 min of AES measurement after exposures up to  $10^{13}$ -L O<sub>2</sub> [1 L (langmuir) =  $10^{-6}$  Torr sec] for sampling a fresh area which had not been irradiated previously by electron beam. The beam-stimulated oxidation, however, occurred during the course of AES or ELS measurements. The Auger peak-to-peak-height ratio of the O signal at 510 eV to the Te signal at 485 eV, which had been initially below the detection limit, increased to 0.014 after 9 min of AES measurement and then to 0.037 after 102 min of the AES and ELS measurements. The (100) surface is more active in oxygen uptake than the (110) surface. The oxygen uptakes of the fresh areas on the ordered surface after the 2-min measurement were  $X_O/X_{Te} = 0.003$ , 0.025, and 0.11 for exposures of  $9 \times 10^9$ -,  $3 \times 10^{12}$ -, and  $1.5 \times 10^{13}$ -L O<sub>2</sub>, respectively. As will be described in the next section, one monolayer coverage of oxygen corresponds to an Auger ratio of  $X_O/X_{Te}$  of about 0.2 for the (100) surface.

Figure 1 shows the loss spectra from the (110) surface for  $E_p$ 's from 50 through 250 eV. Structures called  $E$ , Cd-4*d*,  $\hbar\omega_s$ , and  $\hbar\omega_p$  are of bulk origin<sup>3</sup>;  $E$  is a bulk interband loss, Cd-4*d* is due to the transition from the Cd-4*d* level at 10.5 eV below the valence-band maximum (VBM)<sup>4</sup> to a conduction-band state, and  $\hbar\omega_s$  and  $\hbar\omega_p$  are correlated to the surface- and bulk-plasmon losses, respectively. A structure called  $S$  is of surface origin<sup>3</sup>. The  $S_1$  loss at 4.2,  $S_2$  at 5.8, and  $S_3$  at 10.7 eV are well resolved in the spectrum at  $E_p = 120$  eV. The

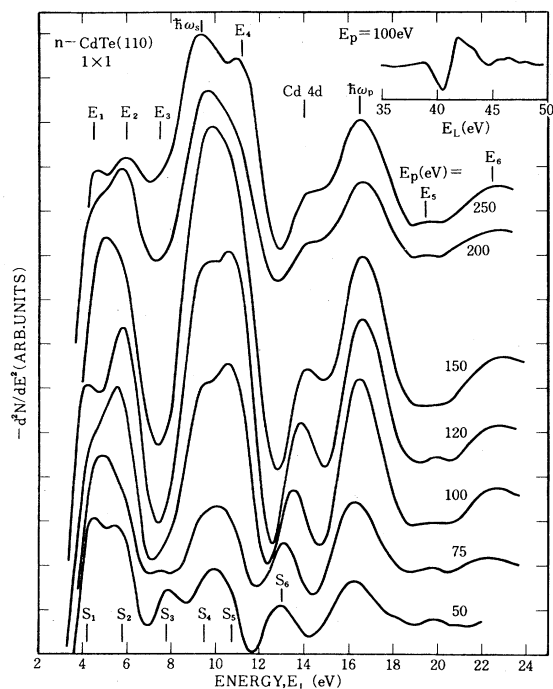


FIG. 1. Electron-energy-loss spectra of the CdTe (110) surface with different primary electron energies;  $E_p = 50, 75, 100, 120, 150, 200,$  and  $250$  eV.

$S_3$  loss at 7.8 and  $S_6$  loss at 13.0 eV are remarkable in the 50-eV spectrum. The  $S_6$  loss has been identified as the transition from the Cd-4d level to the Cd-derived surface state lying at 2.5 eV above the VBM in the one-electron picture free of excitonic effects. The insert in Fig. 1 is the loss spectrum in a region from 35 to 50 eV, which involves the transitions from the Te-4d level. The loss spectrum with  $E_p$  higher than about 120 eV is rather similar in shape among surfaces with different indices. For  $E_p$ 's lower than 120 eV, the spectrum varies with indices or states of the surface because of existence or nonexistence of the surface losses. Figure 2 shows loss spectra from the ordered and disordered (110), (111), and (100) surfaces at  $E_p = 50$  eV. It contains also spectra from the (110) and (100) surfaces with adsorbed oxygen. The surface losses which appeared in each of the spectra are indicated with the sign S in the figure. Their energy positions are summarized in Table I. It should be pointed out that the  $S_1$ ,  $S_5$ , and  $S_6$  losses of the (100) surface are reduced in magnitude drastically upon  $\text{Ar}^+$  bombardment. Simultaneously, the Cd Auger signal decreases in magnitude with respect to the Te Auger signal. This observation indicates that these losses are correlated with the surface Cd atoms. The similar behavior is seen in the spectrum from the (111) surface, although the change

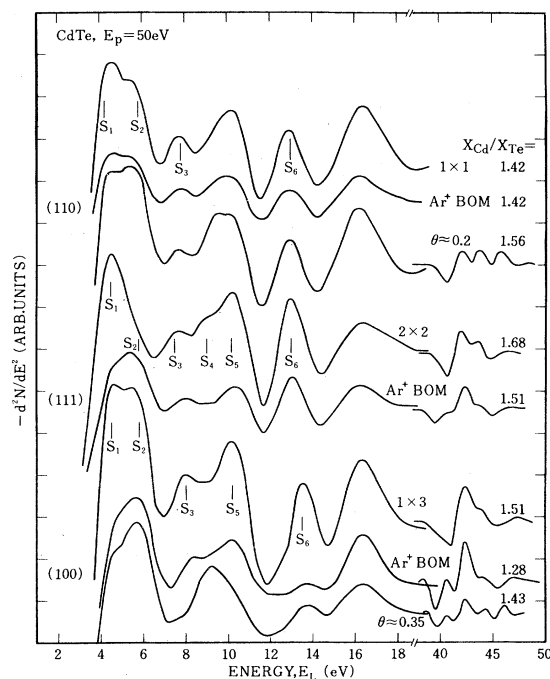


FIG. 2. Electron-energy-loss spectra of the CdTe (110), (111), and (100) surfaces with  $E_p = 50$  eV for loss energies below 20 eV and with  $E_p = 100$  eV in the Te-4d loss region.

in relative magnitude of the structures is not so remarkable as in the case of the (100) surface. The Te-4d losses measured with  $E_p = 100$  eV are included also in Fig. 2, showing that  $\text{Ar}^+$  bombardment produces a loss at 40.5 eV for the (111) and (100) surfaces. A sharp dip at this energy disappears for the disordered (110) and (111) surfaces. This new loss is observed also at the initial stages of oxidation for the (100) surface.

Upon adsorption of oxygen, a loss spectrum changes in shape with appearances of losses due to tellurium oxide (Ref. 3) and disappearances of the features due to CdTe. Changes in a spectrum

TABLE I. Transition energies for surface losses of CdTe (110), (111), and (100) surfaces and their possible identification. Te SS and Cd SS are Te-derived and Cd-derived surface states, CB is a conduction-band state, and Cd-4d is the Cd-4d core level lying at 10.5 eV (Ref. 4) below the valence-band maximum.

	Transition energy (eV)			Possible identification
	(110)	(111)	(100)	
$S_1$	4.2	4.5	4.5	Te SS to Cd SS
$S_2$	5.8	5.8	5.8	
$S_3$	7.8	7.5	8.0	Te SS to CB
$S_4$	9.5	~9		
$S_5$	10.7	10.2	10.2	Te SS to Cd SS
$S_6$	13.0	13.0	13.5	Cd 4d to Cd SS

from the (110) surface is presented in our previous report.<sup>3</sup> It is pointed out that oxidation provides a spectrum similar in shape for surfaces with different indices except at the initial stages of oxidation. Figure 3 shows the spectrum from the (100) surface without (*a* curve) and with adsorbed oxygen (*b-f* curves) at  $E_p = 100$  eV; they were measured on fresh areas before the oxygen exposure (*a* curve) and after the oxygen exposures at  $9 \times 10^9$ - (*b* curve),  $3 \times 10^{12}$ - (*c* curve), and  $1.5 \times 10^{13}$ -L  $O_2$  (*d-f* curves). The spectrum from an  $Ar^+$ -bombarded surface is also included in the figure for comparison. At the initial stages of oxidation (oxygen coverage  $\theta$  is less than about 0.3 of a monolayer), weak losses appear at 3.2, 4.0, 40.5, and 45.8 eV and the losses at 4.5 and 10.9 eV decrease in magnitude, and losses at 5.8 and 9.5 eV increase in magnitude with oxidation. The 3.2- and 40.5-eV losses may be due to disordering the surface caused by adsorption of oxygen. The losses at 6 and 9.5 eV are dominating the others and the shifted Te-4*d* losses grow in magnitude;

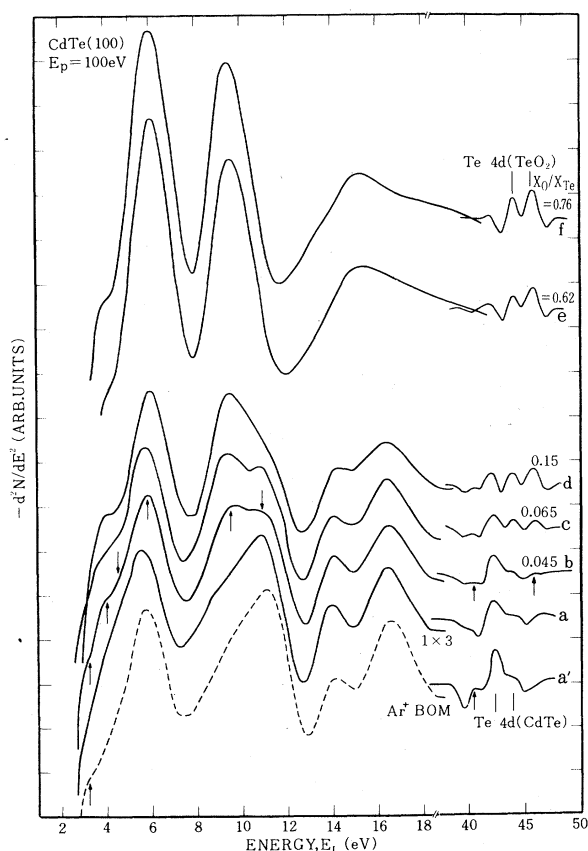


FIG. 3. Electron-energy-loss spectra of the clean ordered (curve *a*), disordered (curve *a'*) and with adsorbed oxygen (curves *b-f*) (100) surfaces of CdTe at  $E_p = 100$  eV.

the features due to CdTe disappear gradually with oxidation for  $\theta \geq 1$ . Finally, the spectrum of the heavily oxidized surface ( $\theta \geq 2$ ) resembles that of  $TeO_2$ . It should be emphasized that the loss spectrum from the heavily oxidized surface taken at  $E_p$  above 250 eV consists of the structures due to both the  $TeO_2$  layer and the CdTe substrate, and that it does not contain such losses as to be correlated with the presence of the Cd element is seen. In the 50-eV spectrum from the (100) surface, the  $S_1$  loss at 4.5 eV and the  $S_5$  loss at 10.2 eV decrease in magnitude with oxidation, as Fig. 2 shows. Figure 3 and the results from the (110) surface indicate that at the initial stages of oxidation the  $S_5$  loss exhibits no significant changes, whereas the shifted Te-4*d* loss appears, suggesting that the oxygen may adsorb preferentially on the surface Te atoms.

#### B. CdSe

The ordered (0001) surface exhibits a  $2 \times 2$  LEED pattern and its opposite (000 $\bar{1}$ ) surface has a  $1 \times 1$  pattern. The oxygen impurity could be reduced to less than 0.01 of a monolayer coverage. While  $Ar^+$  bombardment provided clean surfaces with impurities below detection limits, annealing led to a contamination with K on the (000 $\bar{1}$ ) surface. The Auger peak-to-peak-height ratios of the Cd signal at 380 eV to the Se signal at 42 eV are  $2.38 \pm 0.03$  for the clean ordered (0001) surface and about 2.13 for the  $Ar^+$  bombarded one. The ratio for the annealed (000 $\bar{1}$ ) surface is about 2.3. It is noted that this surface is contaminated but slightly with K. Upon AES and/or ELS measurements the Auger  $X_O/X_{Cd}$  ratio increased to 0.003 for the clean ordered (0001) surface at electron-beam irradiation of 47 min and to 0.009 at 144 min. The  $X_O/X_{Cd}$  ratio of 0.003 corresponds to a coverage of about 0.02 of a monolayer. The beam-stimulated oxidation is more significant for surfaces exposed to molecular oxygen. Although no oxygen Auger signal was observed at the initial stages of the AES measurement on a fresh area after an exposure of  $9 \times 10^8$ -L  $O_2$ , the  $X_O/X_{Cd}$  ratio increased to 0.014 at 4.5 min in the course of the AES measurement and then to 0.021 at 22 min after the measurement of a loss curve. The oxygen uptake of the fresh area on the ordered surface is far less than one monolayer coverage for exposures up to  $10^{14}$ -L  $O_2$ ; the  $X_O/X_{Cd}$  ratio is 0.012 at the exposure of  $1.2 \times 10^{14}$ -L  $O_2$ , which corresponds to a coverage of about 0.08 of monolayer. The oxygen uptake on the (000 $\bar{1}$ ) surface seems to be faster by a factor of ten than on the (0001) surface. It is noticed that the K impurity tends to be eliminated with oxygen uptakes and its Auger signal decreases below the

detection limit on the heavily oxidized surface.

The loss spectrum of the (0001) surface at  $E_p = 100$  eV exhibits large peaks at 3.2, 5.6, 10.7, 14.0, 17.5, and 23.8 eV and a weak shoulder near 7.5 eV, and peaks at 56.4, 61, and 66.2 eV in the Se-3d loss region. The 10.7- and 17.5-eV losses are attributed to the surface- and bulk-plasmon losses,  $\hbar\omega_s$  and  $\hbar\omega_p$ , respectively,<sup>5</sup> and the 14.0-eV loss is related to the transition from the Cd-4d level to the conduction band Cd-4d. The (000 $\bar{1}$ ) surface presents a spectrum similar to that of the (0001) surface except for a weak shoulder near 8.5 eV instead of 7.5 eV. The spectrum with  $E_p$  above 100 eV is rather independent of the primary electron energies. These results indicate that the structures at 3.2, 5.6, and 23.8 eV as well as the Cd-4d loss and the plasmon losses are of bulk origin; they are due to bulk interband losses  $E$ 's. The losses near 7.5 and 8.5 eV may be of surface origin. Surface losses appear more strikingly in the spectrum at  $E_p = 50$  eV. Figures 4 and 5 show the loss spectra from the (0001) and (000 $\bar{1}$ ) surfaces at  $E_p = 100$  and 50 eV, respectively. Figure 5 includes also the spectra from the surfaces with adsorbed oxygen. We will describe detailed effects of oxygen adsorption on the loss spectrum in the next paragraph in this section. As one can see, the spectrum varies in shape between the (0001) and (000 $\bar{1}$ ) surfaces, and it also changes with oxygen uptakes, owing to the presence of surface losses. Peaks at 2.3, 7.2, 8.4, 9.6, 11.5, and 12.7 eV in the 50-eV spectrum may be of surface

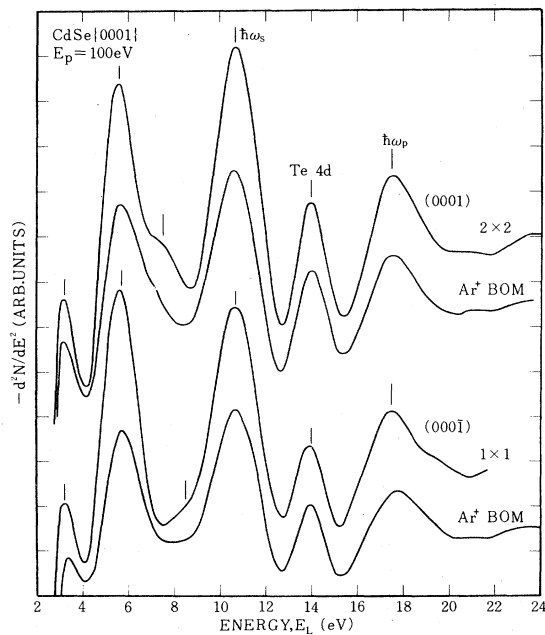


FIG. 4. Electron-energy-loss spectra of the ordered and disordered {0001} surfaces of CdSe at  $E_p = 100$  eV.

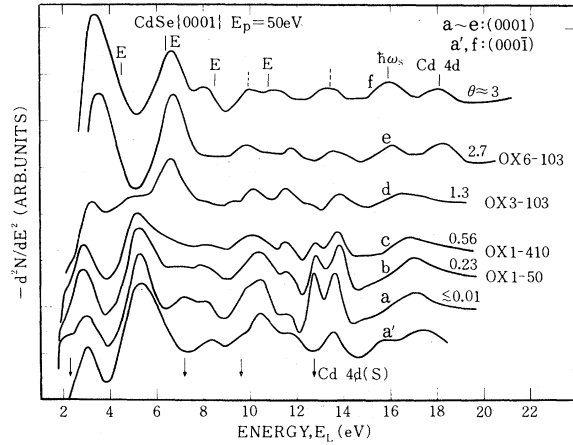


FIG. 5. Electron-energy-loss spectra of the (0001) (curves  $a-e$ ) and (000 $\bar{1}$ ) (curves  $a'$  and  $f$ ) surfaces of CdSe at  $E_p = 50$  eV. The spectra were taken before the oxygen exposure (curves  $a$  and  $a'$ ) and after oxygen exposure (curves  $b-f$ ). Solid lines in the  $f$  curve indicate energy positions of CdO from Ref. 15.

origin. They are absent for the (000 $\bar{1}$ ) surface except for the 11.5-eV loss, indicating they are related to the surface Cd atom. The doublet at 12.7 and 13.6 eV may be associated with the Cd-4d losses; the former peak is due to the Cd-4d surface loss and the latter to the Cd-4d bulk loss. The 12.7-eV loss is very sharp in structure. We emphasize its sharpness, which may reflect an excitonic transition in its origin. The excitonic nature of the transition from a core level to a surface state is widely accepted for semiconductor surfaces.<sup>6,7</sup>

Oxygen uptakes change the shape of the loss spectrum. Before investigating changes occurring at the loss energies  $E_L$ 's below 20 eV, we see change in the Se-3d region (see Fig. 6). At the

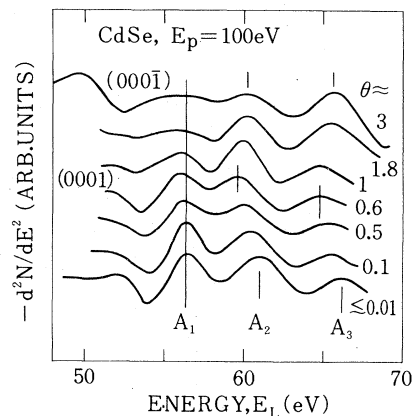


FIG. 6. Electron-energy-loss spectra of clean and with adsorbed oxygen (0001) surfaces and of the very heavily oxidized (000 $\bar{1}$ ) surface of CdSe in the Se-3d region at  $E_p = 100$  eV.

initial stages of oxidation, the 61- and 66.2-eV losses called  $A_2$  and  $A_3$ , respectively, shift to the lower-energy side and locate at 59.6 and 64.8 eV, respectively, at the oxygen coverage of about 0.6 of a monolayer; at this coverage both losses exhibit the maximum shift of 1.4 eV with respect to each of their original positions. For further oxidation, new losses appear at 60.2 and 65.6 eV, where the former becomes small in magnitude and almost disappears for the very heavily oxidized surface. The loss at 56.4 eV,  $A_1$ , gradually reduces in magnitude with oxidation and almost disappears for the heavily oxidized surface. These results indicate that the  $A_1$  loss may be of bulk origin, whereas the other two may be of surface origin. The Auger Se signal at 42 eV reduces in magnitude with oxygen uptakes, and decreases to about 0.20 of its initial magnitude accompanied by an appearance of a dip near 27 eV for the heavily oxidized uptakes, and decreases to about 0.20 of its initial magnitude accompanied by an appearance of a dip near 27 eV for the heavily oxidized surface, as shown in Fig. 7. On the other hand, the Auger Cd signal remains unchanged in magnitude at the very initial stages of oxidation ( $\theta \leq 0.1$ ) tends to decrease slightly ( $\theta \leq 0.6$ ), and then increases for the further oxidation. While the  $A_2$  and  $A_3$  losses shift in position to the lower-energy side, no changes in either the magnitude or in the energy position occur for the Cd-4*d* surface loss for the very initial stages of oxidation ( $\theta \leq 0.1$ ), showing that the oxygen adsorbs preferentially on the sur-

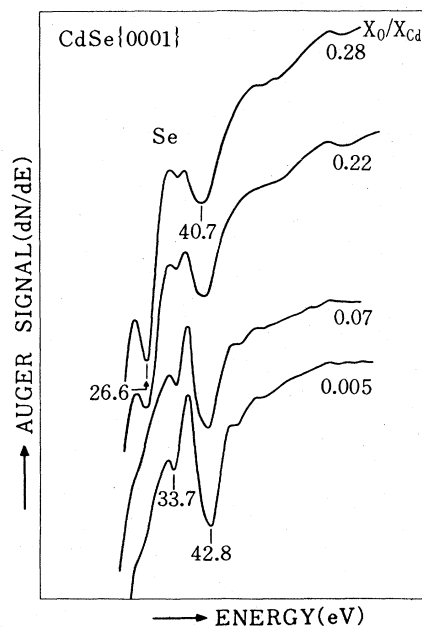


FIG. 7. Auger Se spectra of CdSe surfaces with adsorbed oxygen.

face Se atoms and does not adsorb on the surface Cd atoms at least at the initial oxidation. Further oxidation produces a decrease in magnitude for the Cd-4*d* surface loss and also for the losses at 7.2 and 9.6 eV, as the *b* and *c* curves in Fig. 5 show. These losses diminished in magnitude at oxygen uptakes larger than a monolayer coverage. The oxygen effects on these losses can be explained by the assumption that they are associated with the Cd-derived surface state. We can see in Fig. 5 that the loss spectrum from the surface with oxygen uptakes larger than a monolayer coverage differs drastically in shape from that of the CdSe surface, allowing us to conclude a formation of a bulklike oxide overlayer. The transition energies of the surface losses for CdSe and their possible identification are summarized in Table II.

#### IV. DISCUSSION

##### A. Chemical composition

We attempt to obtain information on the surface chemical composition from the AES data on the basis of a layer model described in our previous paper.<sup>2</sup> Considerations of chemical composition are useful for the study of surface properties. For instance, we can say that the drastic change in loss spectrum between the ordered and disordered (100) surfaces may be correlated primarily to a difference in chemical composition between these surfaces. The layer model yields the intensity of the Cd Auger signal  $X_{Cd}$ , for example, for the (111) Cd surface is proportional to  $I_{Cd}/[1 - \exp(-d/l \cos 42^\circ)]$ , where  $I_{Cd}$  is called the Auger sensitivity of Cd in our previous work,  $l$  the mean free path of the Auger electron, and  $d$  the layer distance given by  $d = a_0/\sqrt{3}$ , using the lattice constant  $a_0$ . Assuming stoichiometry of the nonpolar (110) surface prepared by  $Ar^+$  bombardment

TABLE II. Transition energies for surface losses of the CdSe {0001} surfaces and their possible identification. Cd SS and Se SS are Cd-derived and Se-derived surface states, and Cd-4*d* and Se-3*d* are the Cd-4*d* core level lying at 10.5 eV (Ref. 4) and the Se-3*d* core level lying at 53.1 eV (see text) below the valence-band maximum.

Transition energy (eV)	Possible identification
2.3	Transition to Cd SS
7.2	Transition to Cd SS
8.3	
9.6	Transition to Cd SS
11.5	
12.7	Cd-4 <i>d</i> to Cd SS
61	Se-3 <i>d</i> to Se SS
66.2	Se-3 <i>d</i> to Se SS

and annealing, the model provides the chemical compositions of the ideal (111), ( $\bar{1}\bar{1}\bar{1}$ ), and (100) surfaces, as presented in Table III. As a comparison, it contains the measured values. There is a question of stoichiometry of the bombarded and annealed surface. Very recently we have made AES measurements on a vacuum-cleaved ZnSe (110) surface. The results show that although the Auger ratio of the Se signal at 42 eV to the Zn signal at 55 eV,  $X_{\text{Se}}(42)/X_{\text{Zn}}(55)$  agrees fairly well between the cleaved surface and the bombarded and annealed one, the Auger intensities with respect to the Zn signal at 990 eV,  $X_{\text{Se}}(42)/X_{\text{Zn}}(990)$  and  $X_{\text{Zn}}(55)/X_{\text{Zn}}(990)$  of the cleaved surface are larger than those of the bombarded and annealed surface. This fact indicates that the bombarded and annealed surface is stoichiometric in a relative sense; it is deficient in both the Zn and Se constituents. In the case of CdSe (11 $\bar{2}$ 0) surface, Brillson<sup>8</sup> reported that Ar<sup>+</sup> bombardment produced a surface rich in Se, but annealing could eliminate almost completely surface nonstoichiometry. The chemical compositions investigated in this work are relative, i.e., the surface is called stoichiometric when the Auger ratio of the cation signal to the anion signal has a value corresponding to each of the so-called ideal surfaces, even if the surface is deficient in both the cation and anion. The layer model also can provide the Auger  $X_{\text{O}}/X_{\text{Te}}$  ratio for the one-monolayer coverage of oxygen (one oxygen atom for each of the surface atoms). On the basis of the Auger sensitivity ratios of  $I_{\text{O}}/I_{\text{Zn}}(990)=3.88$  for ZnO and  $I_{\text{Te}}/I_{\text{Zn}}(990)=9.55$  for ZnTe, it provides  $X_{\text{O}}/X_{\text{Te}}=0.19$  and 0.28 for (100) Cd and (110) surfaces, respectively. Comparing the measured value with the calculated one shows that the (111) 2×2 and ( $\bar{1}\bar{1}\bar{1}$ ) 1×1 surfaces are stoichiometric, the (100) 1×3 surface may be a Cd-terminating one with a deficiency of Cd, and the bombarded (100) surface may be a Te-terminating one. Consequently, the drastic

TABLE III. Auger peak-to-peak-height ratios of the Cd signal at 380 eV to the Te signal at 485 eV in CdTe. The experimental values are from the (110) 1×1, (111) 2×2, ( $\bar{1}\bar{1}\bar{1}$ ) 1×1, and (100) 1×3 surfaces, and the calculated ones are obtained by an assumption of stoichiometry of the (110) 1×1 surface (see text).

	$X_{\text{Cd}}/X_{\text{Te}}$	
	Experimental	Calculated
(110)	1.43	
(111)	1.70	1.63
( $\bar{1}\bar{1}\bar{1}$ )	1.25	1.25
(100)	1.50	1.76 (Cd surface) 1.14 (Te surface)

reduction in magnitude of the  $S_{\text{O}}$  loss measured on the disordered (100) surface may be primarily attributed to the change in composition from the ordered surface to the disordered one. It is noticed that there are no significant differences in chemical composition and in the shape of structures in the loss spectrum between the ordered and disordered (110) surfaces. We have shown that in ZnTe the (111), ( $\bar{1}\bar{1}\bar{1}$ ), and (100) surfaces are stoichiometric, and that the (100) 3×1 surface is a Zn-terminating plane. We note that the (100) surface of CdTe has the 1×3 structure, whereas that of ZnTe is the 3×1 structure.

We have not yet examined the nonpolar surface of CdSe and do not have data needed for the consideration of the chemical composition of the polar surface. A measure for the composition, however, can be provided by using the Auger sensitivity ratio  $I_{\text{Cd}}/I_{\text{Se}}$  obtained from the ratios  $I_{\text{Cd}}/I_{\text{Te}}=1.70$  for CdTe,  $I_{\text{Te}}/I_{\text{Zn}}$  for ZnTe, and  $I_{\text{Se}}/I_{\text{Zn}}$  for ZnSe.<sup>2,3</sup> The calculation yields the  $X_{\text{Cd}}/X_{\text{Se}}$  ratios to be 5.3 and 3.6 for the (0001) and (000 $\bar{1}$ ) surfaces, respectively. By similar treatment, the one-monolayer coverage of oxygen on the (0001) surface is given by  $X_{\text{O}}/X_{\text{Cd}}=0.15$ . The measured  $X_{\text{Cd}}/X_{\text{Se}}$  ratio of 2.4 for the (0001) surface is smaller than the calculated one, showing that the CdSe (0001) 2×2 surface is deficient in Cd. We emphasize that in the calculation of the ratio we should take into account a change in shape of the Se signal from ZnSe to CdSe, because in ZnSe the Se signal at 42 eV lies in close to the Zn signal at 55 eV, whereas in CdSe the Se signal is located far away from the other signals. Nonstoichiometry of the CdSe (0001) surface may be compared with the cases of ZnSe and ZnO. That is, we can conclude that the polar surface of the compound having rather ionic bonds seems to be nonstoichiometric, whereas the compound with rather covalent bonds has the polar surface with the stoichiometric composition. Calculations of electrostatic (Madelung potential) surface energies performed by Nosker *et al.*<sup>9</sup> suggest that the polar surface has a stable structure with a nonstoichiometric composition. The surface structures deduced from the LEED pattern and the chemical compositions of the II-IV compounds investigated in the present work are summarized in Table IV, along with the previously reported results.<sup>1-3</sup> The difference in LEED pattern between the *n*- and *p*-type crystals of CdTe may be attributed to unidentified impurities contained in the crystals.

The sticking coefficients of oxygen on the CdTe and CdSe surfaces are extremely small for exposing the well-ordered surface to molecular oxygen. Because of inevitable beam-irradiation effects, we should direct our attention to mini-

TABLE IV. Summary of LEED pattern and stoichiometry of polar surfaces of the zincblende-type compounds of CdTe, ZnTe, and ZnSe and of the wurtzite-type compounds of CdSe and ZnO. The nonpolar (110) or (10 $\bar{1}$ 0) surface of these compounds exhibits a 1 $\times$ 1 pattern. The surface is called stoichiometric (stoichio.) when the measured Auger peak-to-peak ratio of the cation signal (Zn at 55 or Cd at 380 eV) to the anion signal (Te at 485, Se at 42, or O at 510 eV) agrees with the calculated ratio for the corresponding bulk truncated surface on the basis of stoichiometry of the nonpolar surface; otherwise the surface is called nonstoichiometric (nonstoichio.).

(111) or (0001)	( $\bar{1}\bar{1}\bar{1}$ ) or (000 $\bar{1}$ )	(100)
CdTe 2 $\times$ 2, stoichio.	1 $\times$ 1, stoichio.	1 $\times$ 3, Cd surface, nonstoichio.
ZnTe 2 $\times$ 2, stoichio.	1 $\times$ 1, stoichio.	3 $\times$ 1, Zn surface, stoichio.
CdSe 2 $\times$ 2, nonstoichio.	1 $\times$ 1	
ZnSe 2 $\times$ 2, nonstoichio.	(110) facets	5 $\times$ 1, nonstoichio.
ZnO 1 $\times$ 1, nonstoichio.	1 $\times$ 1, stoichio.	

mizing the beam effects in deducing the sticking coefficient of the unexcited oxygen from AES data. A typical beam effect observed in the present work is adsorption of oxygen during the course of AES and ELS measurements. Figure 8 shows the Auger peak-to-peak-height ratios of the O and Se signals to the Cd signal as a function of beam-irradiation period, where the Auger data were taken on a fresh area on the CdSe (0001) surface, and then the surface was exposed to oxygen at an exposure of  $9.1 \times 10^8$ -L O<sub>2</sub>. The  $X_{\text{O}}/X_{\text{Cd}}$  ratio increases sharply at first and then tends to show a saturation after beam irradiation of several hundred minutes. The Se signal at 42 eV remains unchanged in magnitude for the oxygen uptake less than about 0.10 of a monolayer coverage and then decreases gradually for further oxidation. The Cd signal remains unchanged until the oxygen uptake increases to about 0.3 of a monolayer, and then shows a trend of slight decrease and has a magnitude of 0.9 of its initial value at the coverage of about 0.6, which occurs at 450 min after the oxygen exposure. With further oxidation it grows in magnitude and shows an increase of 40% of its initial value for the very heavily oxidized surface. In the case of oxidation

of ZnSe, we observed a remarkable increase in magnitude of the Zn Auger signal for the heavily oxidized surface having a loss spectrum similar to that of ZnO. The initial Auger peak-to-peak height measured within 2 min on the well-ordered CdTe surface shows sticking coefficients  $S \approx 10^{-13}$  for the (100) surface and a value less than  $10^{-14}$  for the (110) surface. The corresponding value for the CdSe (0001) surface is the order of  $S = 10^{-14}$ . We assume that the sticking coefficient thus obtained corresponds to the value free of beam effects. Brillson<sup>8</sup> reported  $S \approx 10^{-13}$  for a vacuum-cleaved CdSe (11 $\bar{2}$ 0) surface using x-ray photoemission spectroscopy.

#### B. Energy-loss spectrum

The transition energies of the bulk losses of CdTe and CdSe surfaces obtained in the present work are in good agreement with results of Henggehold and Pedrotti<sup>5</sup> and of Brillson,<sup>10</sup> as presented in Table V.

Upon Ar<sup>+</sup> bombardment, a new loss appears at the lower-energy side of the Te-4d loss for CdTe, whereas no such loss occurs in CdSe. The Zn

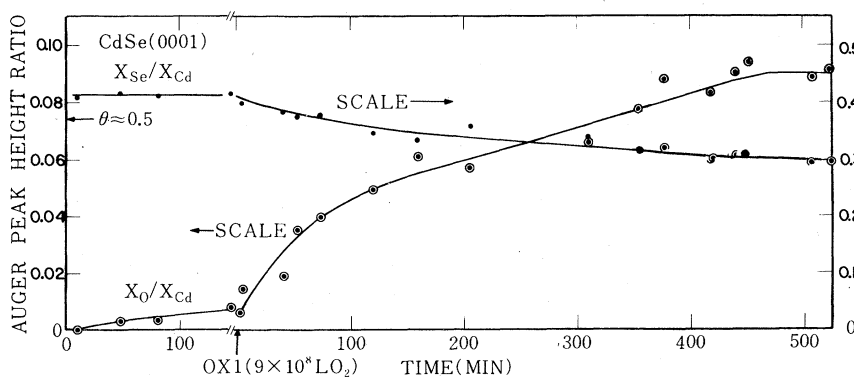


FIG. 8. Auger peak-to-peak-height ratios  $X_{\text{O}}/X_{\text{Cd}}$  and  $X_{\text{Se}}/X_{\text{Cd}}$  as a function of beam-irradiation time before the oxygen exposure and after an oxygen exposure of  $9 \times 10^8$ -L O<sub>2</sub> in CdSe.



TABLE V. Transition energies for bulk interband losses, the surface- and bulk-plasmon losses ( $\hbar\omega_s$  and  $\hbar\omega_p$ ), and the Cd-4*d* and Te-4*d* or Se-3*d* core level losses (Cd-4*d* and Te-4*d* or Se-3*d*) in CdTe and CdSe. For comparison, the ELS results of Hengehold and Pedrotti (HP, Ref. 5) and of Brillson (Ref. 10) are presented.

Present work CdTe (110)	HP CdTe (110)	Remarks
	2.2	
4.5	4.5	
6.0	6.5	
7.5		
9.4	9.6	$\hbar\omega_s$
11.2	10.7	
14.0	13.6	Cd 4 <i>d</i>
16.5	16.1	$\hbar\omega_p$
19.5		
22.5	22.5	
42.0		Te-4 <i>d</i> <sub>5/2</sub>
43.5		Te-4 <i>d</i> <sub>3/2</sub>

Present work CdSe (0001)	HP CdSe (10 $\bar{1}$ 0)	Brillson CdSe (11 $\bar{2}$ 0)	Remarks
3.2	3.0	2.9	
		5	
5.6	6.4	5.6	
		9.5	
10.7	10.7	10.6	$\hbar\omega_s$
14.0	13.8	13.5	Cd-4 <i>d</i>
17.5	17.6	17.5	$\hbar\omega_p$
23.8	23.6		
56.4			Se-3 <i>d</i>

compounds of ZnTe and ZnSe behave in the same way as the Cd compounds<sup>4,2</sup>; we can say that the Te compounds of CdTe and ZnTe exhibit a new Te 4*d* loss at 40.5 eV for both of them upon Ar<sup>+</sup> bombardment, but no new loss appears in the case of the Se compounds. As an origin of the 40.5-eV loss, the presence of the Te element on the bombarded surface might be responsible for this loss. However, comparing the loss spectrum from the disordered surface with that from a Te metal shows that this is probably not the case: Figure 9 shows the loss spectrum of the Te metal measured by the same apparatus used in this work. It has a large peak at 4.6 eV, a weak peak at 7.7 eV, the surface- and bulk-plasmon losses at 11.6 and 17.7 eV, respectively, and a Te-4*d* doublet at 41.1 and 42.6 eV, in fairly good agreement with results reported previously.<sup>11</sup> The energy position of the Te-4*d* doublet is close to that of the 40.5-eV loss, but no other losses characterizing the presence of the Te element are seen in the spectrum from the disordered surface. Consequently, we conclude that the new loss may be correlated to a

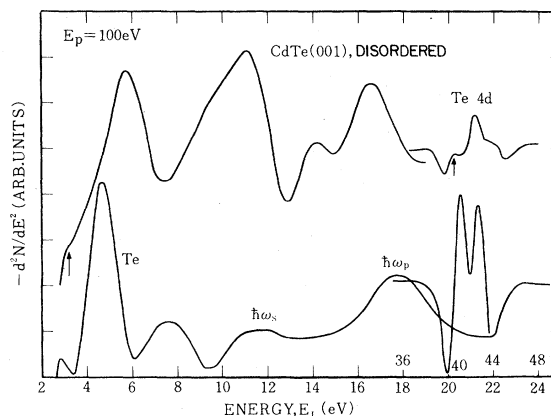


FIG. 9. Comparison of an electron-energy-loss spectra of a Te (10 $\bar{1}$ 0) surface with that of the disordered CdTe (100) surface at  $E_p = 100$  eV.

Te-derived surface state which appeared newly on the disordered surface. It is noted that the loss at 3.2 eV for the disordered CdTe surface may be correlated with the Te-derived surface state.

The disappearance of the  $S_1$  loss and the  $S_5$  loss of the (100) surface of CdTe with oxygen adsorption can be interpreted by a shift in energy of the Te-derived surface states due to adsorption of oxygen on the surface Te atoms. This fact shows that they are associated with Te-derived surface states. We have already indicated that both losses are correlated with the surface Cd atoms. Therefore, we identify the  $S_1$  and  $S_5$  losses as caused by the transitions from the occupied Te-derived surface states lying at  $\sim 1.5$  and  $\sim 7$  eV, respectively, below the VBM to the empty Cd-derived surface state at 2.5 or 3.0 eV above the VBM. The  $S_3$  loss of the (100) surface is also correlated with a Te-derived surface state. These possible identifications for the surface losses are presented in Table I. According to the calculations performed by Calandra and Santoro,<sup>12</sup> occupied surface states of the ideal CdTe (110) surface are located at or near  $\sim 4.5$  and 8.5 eV below the VBM. The former type surface state may be responsible for the  $S_3$  loss and the latter the  $S_5$  loss of the (100) surface.

The energy position of the final state involved in the Se-3*d* loss can be derived from the measured loss energy with a help of the binding energy of the Se-3*d* core level. Vesely and Langer<sup>13</sup> provided the binding energy with respect to the Fermi level; 54.18 and 55.08 eV for the Se-3*d*<sub>5/2</sub> and 3*d*<sub>3/2</sub> levels, respectively, and 11.13 and 12.00 eV for the Cd-4*d*<sub>5/2</sub> and 4*d*<sub>3/2</sub> levels, respectively. The weighted average values are 54.54 eV for the Se-3*d* level and 11.38 eV for the Cd-4*d* level. According to Ley *et al.*<sup>4</sup> the binding energy of the Cd-4*d* level with respect to the VBM is 10.04

$\pm 0.15$  eV, being smaller by 1.44 eV than the value of Vesely and Langer. We assume that this difference is due to the difference in energy reference employed in the two pieces of data, and we subtract it from the value of 54.54 eV to obtain the binding energy of the Se-3*d* level with respect to the VBM. We use the binding energy of 53.1 thus obtained to deduce the final-state energy involved in the Se-3*d* losses, yielding 3.3,  $\approx 8$ , and 13 eV for the  $A_1$ ,  $A_2$ , and  $A_3$  losses, respectively. The level at 3.3 eV may be a conduction-band state, and the other two correspond probably to Se-derived surface states. The loss data can not lead to a conclusion whether the 1.4-eV shift, being measured on the  $A_2$  and  $A_3$  losses upon oxygen adsorption, is attributed to the shift in binding energy of the Se-3*d* core level or to the shift in energy of the final states. According to Pianetta *et al.*,<sup>14</sup> the oxygen chemisorbed on the anion or cation on vacuum-cleaved (110) surfaces of III-V compounds always causes an increase in binding energy of the *d* core level. Therefore it is more likely that the shift in loss energy to the lower-energy side is associated with the shift in energy of the final state; the oxygen adsorbs on the surface Se atoms without breaking the back bonds, resulting in redistribution in charge and a shift in surface states at 8 and 13 eV to the lower-energy side. This assignment seems to be probable for the identification of these losses as due to the transition from the Se-3*d* core level to the surface states, since the adsorbed oxygen may affect more seriously the wave function of the surface state which is less localized on the surface atom than that of the core level which is strongly localized on the surface atom. In this connection, soft-x-ray photoemission studies, which may provide the core-level binding energy, need to be done before definitive conclusions may be drawn. In the case of ZnSe, the Se-3*d* loss with the lowest energy transition corresponds to a bulk loss and the next two lowest losses may result from surface losses. That is, in the Se compounds of CdSe and ZnSe we found the empty anion-derived surface states lying well above the conduction-band minimum (CBM) to which the transitions from the anion core level occur. No corresponding Te-4*d* surface losses are seen in the Te compounds. The final state involved in the Cd surface loss lies at 2.7 eV in the one-electron picture for CdSe, being above the CBM at 1.7 eV where the energy reference is taken at the VBM. This surface loss is sharper in structure than any other *d* core surface loss measured in our laboratory. Owing to a rather poor resolution of our detector, the structure corresponding to this loss measured at 12.7 eV in the 50-eV spectrum, which was measured

with the modulation voltage  $\Delta V$  of 0.2 V peak to peak, may be broadened. We should notice that structure becomes broader at the measurement with  $\Delta V=0.5$  V peak to peak, while no changes in shape are observed for all other structures with the decrease in  $\Delta V$  from 0.5 to 0.2 V peak to peak. Considering the rather-ionic character of chemical bonds in CdSe, the sharpness of the Cd-4*d* surface loss seems to be understandable.

Major features appearing in the spectrum from CdSe surface with the oxygen coverage larger than one monolayer can be explained by the formation of the bulklike CdO layer on the basis of results reported by Hengehold and Pedrotti on a CdO surface.<sup>15</sup> Comparing the loss spectrum from the heavily oxidized CdSe surface with the reported results<sup>15</sup> demonstrates that the losses at  $\sim 4.5$ , 6.6, 7.2, 11.0, 15.9, and 18.1 eV are due to CdO. The energy positions of the losses for CdO from Ref. 15 are indicated by solid lines in the  $f$  curve in Fig. 5. The large loss at 3.3 eV and the losses at 9.9 and 13.4 eV are not seen in Ref. 15. The loss spectrum and the Auger spectrum of the oxidized CdSe surfaces are compared with ELS and AES data taken on clean and oxidized Cd metals, allowing us to conclude that the peak at 3.3, 13.4, and 65.6 eV in the loss spectrum (see Figs. 5 and 6) and the dip near 27 eV in the Auger spectrum (see Fig. 7) of the very heavily oxidized CdSe surface are correlated to CdO. In addition, the comparison with the ELS data yields no evidence for the formation of Cd metal upon oxidation of the CdSe surface. The results for the Cd metal will be reported elsewhere. It is noted that the 65.6-eV loss may be interpreted as due to a transition from the Cd-4*p* level with a binding energy of 70.2 eV with respect to the Fermi level.<sup>13</sup> The transition energy smaller in ELS than the binding energy may be due to excitonic effects in ELS transition. Observations that the 3.3-eV loss grows in magnitude with oxidation and the 13.4-eV loss, which newly appears at the lower-energy side of the Cd-4*d* loss in CdSe and increases in magnitude with the growth of the 65.6-eV loss, do not contradict the present identification. The origin of the 9.9-eV loss is inconclusive. From these considerations we conclude that in the oxidation of CdSe both the cation and anion oxides are involved, although at the first stages of oxidation the anion oxide only is formed and a part of the anion oxide seems to sublime away from the heavily oxidized surface, leaving the oxide overlayer rich in CdO. The presence of the surface Se atoms on the clean (0001) Cd surface is evidenced by the Auger data. As the selenium oxides SeO<sub>2</sub> and Se<sub>2</sub>O<sub>5</sub> are considered from heats of formation,<sup>16</sup> but the formation of SeO<sub>2</sub> may be more

probable because there may not be sufficient oxygen for the formation of  $\text{Se}_2\text{O}_5$ , or owing to such a high vapor pressure as  $1.4 \times 10^{-6}$  Torr at room temperature,<sup>16</sup>  $\text{SeO}_2$  may sublime away from the surface when oxidation proceeds to  $\text{SeO}_2$ .

The oxidation behavior of the CdSe surface seems to be interpreted by a model similar to that proposed by Pianetta *et al.*<sup>14</sup> for the GaAs (110) surface. The oxygen adsorbs on the surface Se atoms without breaking the back bonds at the initial stages of oxidation with oxygen coverage  $\theta$  less than about 0.6 of a monolayer. The Cd-4*d* surface loss remains unchanged at  $\theta \leq 0.1$  and then decreases in magnitude with further oxidation. The oxygen adsorbed on the surface Se atoms may produce a shift in energy of the empty Cd-derived surface state, following theoretical calculations of the density of states for the GaAs (110) surface with adsorbed oxygen on various surface species reported by Mele and Joannopoulos.<sup>17</sup> Subsequent addition of the excited oxygen leads to breaking the back bonds and the oxygen adsorbs on the surface Cd atoms as well as on the surface Se atoms and both the cadmium and selenium oxides are formed at  $\theta \geq 0.6$ . Further exposures to excited oxygen cause the oxidation to proceed into the bulk ( $\theta > 1$ ), leading to the changes in shape of both the loss spectrum and Auger spectrum in the region below 50 eV. The decrease in magnitude of the Auger Se signal at 42 eV indicates a decrease in composition of the Se constituent in the oxide overlayer. In addition, changes in shape of the Auger signal from CdSe to selenium oxide may produce the decrease. In fact, in the case of Te metal, the Te Auger signal at 25 eV has a magnitude of about 0.4 of that of the Te signal at 485 eV, whereas the Te signal at 25 eV almost disappears in the tellurium oxide. The appearance of the Cd signal due to CdO at about 27 eV may have effects also on the magnitude of the Se signal at 42 eV. There is another measure for the chemical composition of the oxide overlayer. The maximum Auger ratio  $X_{\text{O}}/X_{\text{Cd}}$  was 0.31 for the very heavily oxidized CdSe surface, in good agreement with a value measured for the heavily oxidized Cd metal. Consequently, we conclude that the selenium oxide sublimates away from the oxide overlayer, leaving the overlayer rich in CdO. In the case of the oxidation of ZnSe, both the Auger Se signal and Se-3*d* loss are reduced in magnitude without changes in shape with oxygen uptakes and they almost disappear for the heavily oxidized surface, indicating that the selenium oxide sublimates from the surface, resulting in a oxide overlayer composed entirely of ZnO.

Comparing the loss spectrum from the oxidized CdTe surface with that from the oxidized CdSe

surface allows us to conclude that no cation oxide is involved in oxidation of CdTe. At the oxidation of CdTe, the appearance of the Te-4*d* loss due to  $\text{TeO}_2$  at the very initial stages of oxidation (see curve *b* in Fig. 3) demonstrates that the oxygen adsorbs on the surface Te atoms with breaking the back bonds from the initial stages of oxidation, leading to the formation of  $\text{TeO}_2$ . No evidence for a formation of the Cd element is seen in the loss spectrum. Due to its high vapor pressure,<sup>18</sup> the Cd element, which may appear as a reduced element upon the formation of  $\text{TeO}_2$ , may sublime from the oxide overlayer. The Auger ratio  $X_{\text{Te}}/X_{\text{O}}$  was 1.53 for the heavily oxidized CdTe surface. Owing to desorption of oxygen during the course of AES and ELS measurements, no reliable Auger ratio was obtained for the  $\text{TeO}_2$  crystal; the  $X_{\text{Te}}/X_{\text{O}}$  ratio changed from 1.20 measured immediately after beam irradiation to 1.58 after AES and ELS measurements. The layer model shows it to be 1.23, as deduced from an assumption that the ratio is given by a half of the sensitivity ratio of  $I_{\text{Te}}/I_{\text{O}}$ , which can be provided by the values for  $I_{\text{Zn}}/I_{\text{Te}}$  in ZnTe and  $I_{\text{Zn}}/I_{\text{O}}$  in ZnO. The estimated value is in good agreement with the initially measured one. We emphasize, however, that the estimation yields a measure for the Auger ratio, because of no consideration of the crystal structure of  $\text{TeO}_2$  and of a change in shape of the Auger spectrum due to the close location of the Te and O signals.

We have already shown that in oxidation of ZnTe<sup>2</sup>, both ZnO and  $\text{TeO}_2$  are involved in the oxide overlayer. The Te-4*d* loss due to  $\text{TeO}_2$  is seen at an oxygen coverage of about 0.5 of a monolayer, whereas the 40.5-eV loss appears at the very initial stages of oxidation. The 40.5-eV loss has been identified as due to the transition from the Te-4*d*<sub>5/2</sub> level to the Te surface state lying  $\sim 0.3$  eV above the VBM in a one-electron picture.<sup>2</sup> Mele and Joannopoulos have indicated in their calculation of the surface states for the GaAs (110) surface that an anion-derived empty surface state appeared in the band-gap region with adsorption of oxygen on the surface anion atoms.<sup>17</sup> The similar oxygen-induced surface state may be responsible for the 40.5-eV loss in ZnTe. The Zn-3*d* surface loss in ZnTe diminished in magnitude with oxygen uptakes at the rather initial stages of oxidation due to a disappearance of the empty Zn-derived surface state. The observation on the Te 4*d* loss indicates that the oxygen adsorbs on the surface Te atoms, probably, without breaking the back bonds at the initial stages of oxidation. The observed result on the Zn-3*d* loss may also provide another evidence for the adsorption of the oxygen on the surface Te atoms according to the calcula-

tion of Mele and Joannopoulos,<sup>17</sup> but a possibility of the adsorption of the oxygen on the surface Zn atoms can not be ruled out completely. Calculations of the surface states for the surface with adsorbed oxygen seem to be needed before definitive conclusions are drawn.

We have found from the ELS and AES studies that both the anion and cation oxides are involved in the oxide overlayer developed on the CdSe, ZnTe, and ZnSe surfaces, and only the anion oxide is formed in the case of CdTe: The anion oxide is formed without exception in all the II-VI compounds investigated by us. These oxidation properties seem to be explained on the basis of heats of formation for each of the oxides involved (see Fig. 10).<sup>16,18</sup> We can see from Fig. 10 that both the anion and cation oxides are more stable than the corresponding Cd (and Zn) selenide or telluride and that the cation oxide is involved in addition to the anion oxide only when it is more stable than the corresponding anion oxide, if SeO<sub>2</sub> is involved as the selenium oxide. If Se<sub>2</sub>O<sub>5</sub>, which is more stable than SeO<sub>2</sub>, is formed as the selenium oxide, sublimation of selenium oxide may be responsible for the formation of the cation oxide. In this connection, oxidation of the Zn and Cd sulfides may provide more useful information on the oxidation properties of the II-VI compound surfaces.

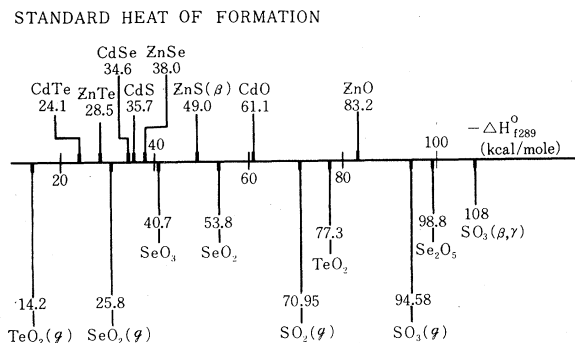


FIG. 10. Standard heats of formation from Refs. 16 and 18 for the Cd and Zn calcogenides and their anion and cation oxides in the solid state and for some anion oxides in the gaseous state.

#### ACKNOWLEDGMENTS

We would like to thank Professor Y. Nishina for supplying vapor-phase grown Te single crystals. This work was supported in part by Grants in Aid for Scientific Research from the Ministry of Education, Science and Culture of Japan, and by the Toray Science Foundation of Japan.

<sup>1</sup>A. Ebina and T. Takahashi, Phys. Rev. B **16**, 2676 (1977).

<sup>2</sup>A. Ebina, K. Asano, and T. Takahashi, Phys. Rev. B **18**, 4332, 4341 (1978).

<sup>3</sup>A. Ebina, K. Asano, and T. Takahashi, Surf. Sci. **86**, 803 (1979).

<sup>4</sup>L. Ley, R. A. Pollak, F. R. McFeely, S. P. Kowalczyk, and D. A. Shirley, Phys. Rev. B **9**, 600 (1974).

<sup>5</sup>R. L. Hengehold and F. L. Pedrotti, Phys. Rev. B **6**, 2262 (1972).

<sup>6</sup>W. E. Spicer, P. Pianetta, I. Lindau, and P. W. Chye, J. Vac. Sci. Technol. **14**, 885 (1977).

<sup>7</sup>R. S. Bauer, J. Vac. Sci. Technol. **14**, 899 (1977).

<sup>8</sup>L. J. Brillson, Surf. Sci. **69**, 62 (1977).

<sup>9</sup>R. W. Noskar, P. Mark, and J. D. Levine, Surf. Sci. **19**, 291 (1970).

<sup>10</sup>L. J. Brillson, Phys. Rev. B **18**, 2431 (1978).

<sup>11</sup>S. Andersson, D. A. Andersson, and I. Marklund,

Surf. Sci. **12**, 284 (1968).

<sup>12</sup>C. Calandra and G. Santoro, J. Vac. Sci. Technol. **13**, 773 (1976).

<sup>13</sup>C. J. Vesely and D. W. Langer, Phys. Rev. B **4**, 451 (1971).

<sup>14</sup>P. Pianetta, I. Lindau, C. M. Garner, and W. E. Spicer, Phys. Rev. B **18**, 2792 (1978).

<sup>15</sup>R. L. Hengehold and F. L. Pedrotti, J. Appl. Phys. **47**, 287 (1976).

<sup>16</sup>K. C. Mills, in *Thermodynamic Data for Inorganic Sulphides, Selenides, and Tellurides* (Butterworths, London, 1974).

<sup>17</sup>E. J. Mele and J. D. Joannopoulos, Phys. Rev. B **18**, 6999 (1978).

<sup>18</sup>*Handbook of Chemistry and Physics*, edited by R. C. Weast (The Chemical Rubber Company, Cleveland, Ohio, 1972).